RSC Advances

PAPER

View Article Online
View Journal | View Issue

Cite this: *RSC Adv.*, 2025, **15**, 29462

pH-responsive release of small molecule pharmaceuticals from a reworked adsorbent hydrogel for environmental applications

Hitarth Patel,[a] Rinki Singh *[a] and Bhaskar Datta *[ab]

Hydrogels that are engineered for environmental and biomedical applications possess an overlapping set of material and surface properties. In this work, we have repurposed a poly(acrylic acid-*co*-vinyl sulfonic acid) (PAcVSA) hydrogel that has been previously used for organic dye removal, for the pH-sensitive release of small molecule pharmaceuticals. The engineered PAcVSA hydrogel displayed highly pH-sensitive swelling behaviour with a percentage swelling of 6000% or more in the pH range of 5–8. The known pharmaceutical sulfadiazine (SDA) and an indigenously developed small molecule pharmaceutical (TBS), displayed pH-responsive cumulative release of 82.1% and 80.6% of SDA and TBS, respectively, at pH 5 over 24 h. The difference in cumulative release percentage of the small molecules from PAcVSA at pH 5 and pH 8 is superior compared to other reported pH-responsive synthetic hydrogels. The kinetic modelling of release from the loaded PAcVSA hydrogels suggests different mechanisms underlying release, with Fickian diffusion for SDA and polymer relaxation for TBS. This work represents the successful cross-use of an adsorbent hydrogel relevant for environmental remediation, towards the distinctive carry and release of small molecule pharmaceuticals.

Received 29th May 2025
Accepted 29th July 2025

DOI: 10.1039/d5ra03794h

rsc.li/rsc-advances

1. Introduction

Polymeric hydrogels have attractive applications in the apparently unrelated contexts of trapping hazardous agents and delivery of drugs.[1–3] pH-responsive hydrogels are stimuli-responsive materials that are sensitive to the pH of the surrounding medium.[4] Hydrogels responsive to temperature, ionic strength and concentration of glucose exemplify other types of stimuli-responsive behaviour.[5–7] The ability of hydrogels to control the uptake or release of analytes in dynamic response to the surrounding medium is valuable for environmental or biomedical applications.[2,8] Notably, disease conditions in humans can produce changes in the physiological environment in a spatio-temporal manner.[9,10] The release profile of drugs from stimuli-responsive hydrogels can be tuned to optimize bioavailability and efficacy.[11] Stimuli-responsive hydrogels can be designed to respond to specific environmental cues, such as pH, light, magnetic fields, electricity, or biological factors, and perform targeted functions.[12,13] Poly(acrylic acid) (PAc) is a prominent constituent of pH-responsive hydrogels. The inclusion of other pH-responsive components such as poly(vinyl sulfonic acid) (PVSA) has sought to expand on the pH-sensitivity of the resulting hydrogels.[14,15] Hydrogels comprising PAc and PVSA have been reported previously for the adsorption of methylene blue dye from aqueous solutions.[16] PAc displays high drug storage and delivery capabilities and is attractive for its nontoxic behaviour.[17] Polymers comprising acrylic acid have been separately reported for drug delivery and dye adsorption. Notably, Ujwala *et al.*, developed sodium alginate, acrylic acid, 2-acrylamido-2-methyl-1-propane sulfonic acid and locust bean gum microbeads for pH-responsive release of doxorubicin, while Chen *et al.*, used acrylic acid, tea polyphenol and chitosan hydrogel for curcumin delivery.[18,19] On the other hand, Wu *et al.*, and Singh *et al.*, reported acrylic acid hydrogels for MB dye adsorption.[20,21] The present study addresses three distinct research gaps. First, while hydrogels have been widely reported in the unrelated domains of environmental and biomedical applications, there is a dearth of synthetic hydrogels that can be cross-used across the domains. This dearth of reports is felt even more sharply upon benchmarking the performance of the synthetic hydrogel *vis-à-vis* other synthetic and biopolymer composite hydrogels.[22] Second, while acrylic acid is a prominent constituent of hydrogels, there are no reports of synthetic poly(acrylic acid)-based hydrogels being used both for environmental mitigation and for release of small molecule drugs. Existing drug-releasing hydrogels comprising poly(acrylic acid) rely on the use of prominent biopolymers.[23,24] Third, differences in the mechanism of release of different small molecule drugs from the same hydrogel are rarely scrutinized. This creates a lacuna in understanding the

[a]*Department of Chemistry, Indian Institute of Technology Gandhinagar, Palaj, Gandhinagar, 382355, Gujarat, India. E-mail: bdatta@iitgn.ac.in; rinkoosingh62@gmail.com*

[b]*Department of Biological Sciences & Engineering, Indian Institute of Technology Gandhinagar, Palaj, Gandhinagar, 382355, Gujarat, India*

scope of use of drug-releasing hydrogels considering that the discovery of small molecule drugs routinely depends on modifying or adapting the chemical scaffolds of established drugs. This study addresses the above gaps by demonstrating the distinctive small molecule drug-releasing behaviour of poly(acrylic acid-*co*-vinyl sulfonic acid) or PAcVSA, a synthetic hydrogel that has already been reported previously for its attractive cationic dye adsorption properties.[20,21] A pH-responsive PAcVSA hydrogel was loaded with two different small molecules sulfadiazine (SDA) and a triaryl benzenesulfonamide (TBS), that represent an established pharmaceutical agent and a scaffold displaying potent pharmaceutical activity.[25–28] The release of these molecules from PAcVSA was accompanied by one of the best reported cumulative release percentages, different mechanisms of release and a superlative pH-responsive behaviour of the hydrogel. To the best of our knowledge, this work represents the first crossover application of an environmentally relevant adsorbent hydrogel as a carrier for release of small molecules and pharmaceutical agents.

2. Materials and methods

2.1 Materials

Acrylic acid (Ac) and vinyl sulfonic acid (VSA) as monomers were purchased from Sigma Aldrich (Bangalore, India), along with ammonium persulfate (APS) (Sigma Aldrich, Bangalore, India) and Ethylene glycol Di methacrylate (EGDMA) (Alfa Aesar, Bangalore, India) as initiator and crosslinker respectively for the synthesis of poly(acrylic acid-*co*-vinyl sulfonic acid), (PAcVSA) hydrogel. For the synthesis of triaryl thiazolyl benzenesulfonamide (TBS) molecules, thioanisole, phenyl acetyl chloride, aluminium trichloride, hydrogen peroxide, and hydrogen bromide were used and purchased from Sigma Aldrich (Bangalore, India) and thiourea and 4-bromo-2-fluorobenzenesulfonyl chloride were purchased from Tokyo Chemical Industry (Hyderabad, India). Sulfadiazine which was used as a reference molecule was purchased from Tokyo Chemical Industry (Hyderabad, India). Human embryonic kidney (HEK293T) cells were procured from National Centre for Cell Science (NCCS) Pune, India.

2.2 Preparation of poly(acrylic acid-*co*-vinyl sulfonic acid) hydrogel

The pH-sensitive poly(acrylic acid-*co*-vinyl sulfonic acid) hydrogel PAcVSA was synthesized by the free radical polymerization method reported in the literature with some modifications.[16] 1.491 g of acrylic acid (Ac) and 1.148 g of vinyl sulfonic acid (VSA), corresponding to an optimized weight ratio as reported in the literature, were transferred into a 100 ml beaker. The mixture was magnetically stirred at room temperature (25 °C) for 10 min to ensure homogenous blending. 0.0105 g of ethylene glycol dimethacrylate (EGDMA) was added as the crosslinker to the monomer solution, and the mixture was stirred for another 10 min to ensure uniform dispersion. 0.0148 g of ammonium persulfate (APS) was added to the reaction mixture under continuous stirring for 5–10 min to ensure thorough mixing of the initiator. Milli-Q water was gradually added to the mixture while stirring to bring the total weight of the solution to 5 g. The final solution was stirred for 1 h at room temperature to achieve a uniform reaction mixture. Nitrogen gas was bubbled through the solution for 1 h to eliminate dissolved oxygen and air bubbles that could inhibit polymerization. The degassed solution was transferred into a reaction vessel and placed in a water bath maintained at 60 °C. The polymerization was allowed to proceed for 45 min until gelation was complete. After gelation, the hydrogel was allowed to cool to room temperature. The hydrogel was removed from the reaction vessel and washed thoroughly with a 50 : 50 (v/v) ethanol–water mixture to remove unreacted monomers. The washed hydrogel was dried in a hot air oven at 60 °C until a constant weight was obtained. The dried hydrogel was stored in a vacuum desiccator until further use.

2.3 Characterization of PAcVSA hydrogel

For the detailed characterization of hydrogel before and after adsorption of small molecules, powders of dried PAcVSA, PAcVSA_SDA and PAcVSA_TBS were prepared using mortar-pestle followed by drying in a hot air oven at 60 °C. Fourier Transform Infrared (FTIR) spectra of the oven dried powder of pristine PAcVSA, PAcVSA_SDA, and PAcVSA_TBS were recorded with an attenuated total reflectance (ATR) accessory in transmission mode using a PerkinElmer Spectrum Two spectrophotometer. The spectra were recorded between 4000 and 400 cm^{-1} at 4 cm^{-1} resolution at room temperature. Thermogravimetric Analysis (TGA) of TBS, SDA, and oven dried powders of pristine PAcVSA, PAcVSA_SDA, and PAcVSA_TBS hydrogels were evaluated by using a NETZSCH STA 449F3 instrument with a 10 °C min^{-1} rate ranging from 30 °C to 500 °C. Powder X-ray diffraction studies of oven dried powders of pristine PAcVSA, PAcVSA_SDA and PAcVSA_TBS hydrogels were carried out using Bruker D8 discover diffractometer with Cu Kα radiation of 1.54 Å at room temperature. The surface morphology of freeze-dried pristine PAcVSA, PAcVSA_SDA, and PAcVSA_TBS hydrogels were studied by field emission scanning electron microscopy (FESEM), on a JEOL 7900F at room temperature. For the FESEM analysis the freeze-dried hydrogel samples were plasma coated for 90–120 s in a gold-based sputter coater under argon environment. For the rheological study of pristine PAcVSA, PAcVSA_SDA, and PAcVSA_TBS, initial swelling of the pristine hydrogels were performed in DI water at neutral pH. The rheological study of pristine PAcVSA, PAcVSA_SDA and PAcVSA_TBS hydrogel were performed using MCR 702 Anton Paar Rheometer at normal room temperature.

2.4 pH-responsive swelling behaviour of PAcVSA hydrogel

To study the swelling behaviour of PAcVSA, the measurements of swelling characteristics and swelling ratio of the prepared PAcVSA hydrogel were studied at pH 5, 7.4 and 8. The gravimetric method was used to determine the hydrogel sample's swelling ratio.[29,30] Briefly, 110 mg of hydrogel sample was placed inside a weighed tea bag and submerged in 100 mL of different pH buffer solutions at room temperature. After soaking for

a predetermined time interval for 96 h the tea bag containing swollen hydrogel was wiped off with filter paper and weighed. The swelling ratio (%) at different pH were measured at least in triplicate and the mean and standard error were calculated.

2.5 Small molecule loading in the PAcVSA hydrogel

The commercially available Sulfadiazine (SDA) and indigenously synthesized triaryl thiazolyl benzenesulfonamide (TBS) were used as small molecules for the loading and release study. In a typical procedure, 100 mg of dried PAcVSA hydrogel was immersed in 5 mg in of each SDA and TBS solutions [prepared in 30 mL of ethanol : water (1 : 1)] at 37 °C and shaken at 100 rpm. After 48 h of incubation the hydrogel was carefully removed from the drug solution, washed with DI water, and dried in an oven at 60 °C for 48 h. The amount of the drug-loaded in PAcVSA hydrogel were calculated according to the original concentration of the drug molecules and the concentration the drugs in the solution after loading, which was quantified by UV-visible spectroscopy (JASCO V-750 spectrophotometer) *via* absorbance at wavelength 277 nm (SDA) and 304 nm (TBS), respectively. Standard calibration curves for SDA and TBS molecule solutions are shown in Fig. 1d and e.

2.6 *In vitro* drug release from PAcVSA hydrogel

About 100 mg of drug-loaded dried hydrogels, namely PAcVSA_SDA and PAcVSA_TBS, were immersed in 100 mL of different pH buffer solution (pH 5, pH 7.4 and pH 8) in a 250 mL beaker. The beakers were placed on a water bath at 37 °C under constant stirring at 250 rpm. At a preplanned time point, the released media were collected and replaced with 1 mL of fresh buffer solution. The released TBS and SDA released were quantified by UV-visible spectroscopy, all results were collected through three parallel samples. The cumulative release percentage was calculated by eqn (1).

$$\text{Cumulative release (\%)} = \frac{\text{amount of drug released}}{\text{amount of drug encapsulated in hydrogel}} \times 100 \quad (1)$$

2.7 Kinetics of small molecule release from PAcVSA hydrogel

In order to evaluate the release kinetics of TBS and SDA from PAcVSA hydrogel, all collected data were fitted to different kinetic models, (1) zero-order model, (2) first-order model, (3) Higuchi model, (4) Korsmeyer–Peppas model, and (5) Hixon–

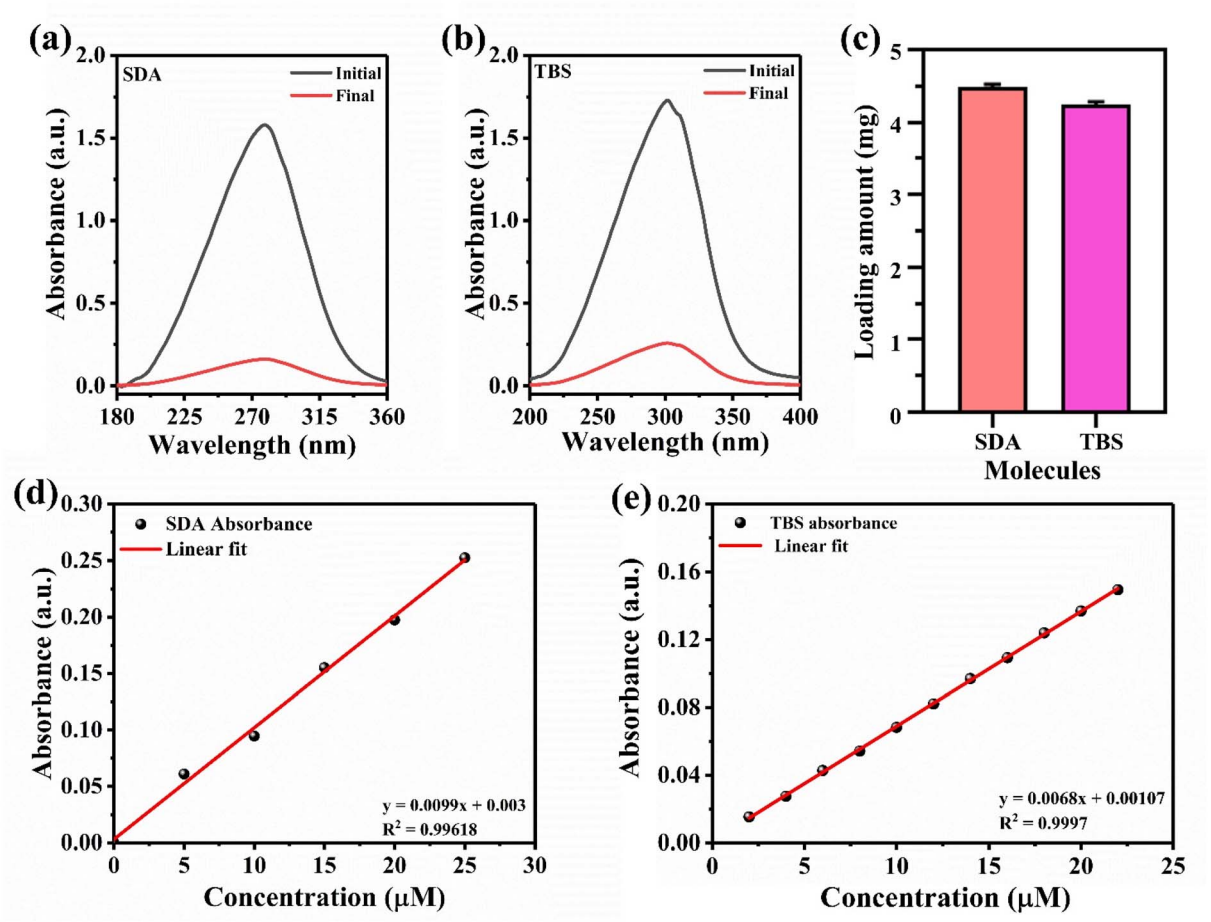

Fig. 1 UV spectrum of (a) SDA and (b) TBS before and after loading, (c) amount of drug loading on PAcVSA hydrogel, and calibration plots of (d) SDA and (e) TBS.

Crowell model.[31–33] The best kinetic fit for drug release from the TBS and SDA-loaded hydrogels were estimated by comparing the performance of the five models. The equations underlying each of the five models tested are described here.

(1) Zero-order model: this describes drug release from a polymeric matrix that is independent of the drug concentration within the matrix,[34,35] and can be represented by eqn (2),

$$Q_t = Q_0 + k_0 t \quad (2)$$

where Q_t represents the amount of drug released from polymeric matrix, Q_0 is the initial amount of drug present in the solution, k_0 is the zero-order rate constant in concentration/time, and t is time. Zero-order kinetics refers to a process in which a drug is released at a constant rate from a polymeric matrix.

(2) First-order model: the release rate of drugs from the polymeric matrix in the first-order model is dependent on the drug concentration[34,35] and the model can be depicted by eqn (3),

$$\log Q_t = \log Q_0 - kt/2.303 \quad (3)$$

where Q_t is the amount of drug released at time t, Q_0 is the initial amount of the drug in the matrix at time $t = 0$, and k is the rate constant expressed in time.

The speed at which a drug is released from a polymeric matrix increases as the concentration of the drug in the matrix increases. The value of correlation coefficient value obtained from the linear plot corresponding to eqn (3) helps in determining the goodness of fit of the first-order model for the drug release from polymeric matrix.[35,36]

(3) Higuchi model: the Higuchi model depicts drug release from the polymeric matrix as a square root function of time, based on Fick's law of diffusion,[35,36] and can be expressed as eqn (4),

$$Q_t = kt^{0.5} \quad (4)$$

where k is constant.

A plot of the cumulative percentage of drug release on the y-axis and the square root of time on the x-axis can be used for estimation of the correlation coefficient. A higher value of the correlation coefficient indicates that the diffusion control mechanism is responsible for the drug release from the polymeric matrix.[36]

(4) Korsmeyer–Peppas model: this model seeks to provide precise mechanistic insight into the drug release from controlled-release polymer systems,[35,36] and can be expressed as eqn (5),

$$Q_t = Kt^n \quad (5)$$

where Q_t is the amount of drug released from the polymeric matrix, K is constant corresponding to the structural and geometric characteristics of the matrix and n is the releasing exponent. The value of n determines the type of diffusion mechanism. The Fickian diffusion mechanism occurs if ($n \leq 0.43$), while the anomalous or non-Fickian diffusion mechanism occurs if ($0.43 > n > 0.85$). For ($n > 0.85$), the release of the drug from the polymeric matrix is followed by super case II.[36–38]

(5) Hixson–Crowell model: this model explains drug release from the polymeric matrix based on induced voids that change surface area.[34,38,39] The relation between drug release and time can be expressed as,

$$W_0^{1/3} - W_t^{1/3} = K_{hc} t \quad (6)$$

where W_0 is the initial amount of drug, W_t is the amount of drug at any time t, and K_{hc} is the Hixson–Crowell constant.

2.8 Cell proliferation assay

The *in vitro* cytotoxicity of the PAcVSA hydrogel on human embryonic kidney HEK 293T cells was evaluated by an MTT assay. The prepared PAcVSA hydrogel was sterilized by using 70% ethanol, followed by UV irradiation. The PAcVSA hydrogel was then equilibrated in freshly prepared and sterile phosphate-buffered saline (PBS) solution (1.5 mL per well) for 1 h in 12-well plates. After 1 h, PBS was aspirated and hydrogels weighing 1, 2, 3, 4, and 5 mg were placed in the DMEM media (1.5 mL per well) supplemented with 10% FBS, 1% penicillin/streptomycin, and incubated overnight for 37 °C. HEK 293T cells (10 000 cells per well, 1.5 mL DMEM medium) were seeded on the hydrogels after the used medium was removed from the plates and replaced with 0.5 mg mL^{-1} of 1.5 mL per well MTT solution. After incubation for 4 h the medium was aspirated and replaced with DMSO to solubilize formazan crystal. The optical density (OD) of the samples were measured at 570 nm using a PerkinElmer microplate reader. Control cells were cultured only in cell culture medium without addition of the hydrogel. All experiments were conducted at least in three replicates.[40]

2.9 Live/dead cell assay

The cytotoxicity of PAcVSA hydrogel on human embryonic kidney HEK293T cells was also assessed by fluorescence staining using calcein AM and propidium iodide.[41] Sterilization of the prepared PAcVSA hydrogel was first performed with 70% ethanol followed by UV irradiation. The PAcVSA hydrogel was placed in 12 well plates as described above. Subsequently, HEK 293T cells (10 000 cells per well, 1.5 mL medium) were seeded on the hydrogels after the used medium was removed from the plate. After 72 h of incubation the cells were stained with 500 nM calcein Am (excitation: 485 nm) and 500 nM propidium iodide (excitation: 530 nm) dye for 20 min followed by washing with fresh DMEM media. The cells were imaged using a confocal laser scanning microscope to determine the viable cells.[41]

3. Results and discussion

The pH-sensitive PAcVSA hydrogel was synthesized by free radical polymerization as described in the Experimental section and depicted in Fig. S1. The PAcVSA hydrogel was synthesized with an optimized weight ratio of 5 : 1 of acrylic acid (Ac) and

vinyl sulfonic acid (VSA), based on the ability of the higher proportion of Ac to self-bridge by cross-linking.[16] We used ethylene glycol di-methacrylate as a crosslinking agent. Based on the prospective mechanism of hydrogel formation, the vinyl sulfonic acid (SO_3^-) of VSA and the carboxylate (COO^-) group of Ac may exert substantive electrostatic interactions with the sulphonamide small molecules being used, thereby increasing their likelihood of sustained absorption or trapping in aqueous environment.

3.1 Synthesis of 4-bromo-2-fluoro-*N*-(4-(4-(methylsulfonyl) phenyl)-5-phenylthiazol-2-yl) benzenesulfonamide (TBS)

4-Bromo-2-fluoro-*N*-(4-(4-(methylsulfonyl)phenyl)-5-phenylthiazol-2-yl) benzenesulfonamide was synthesized based on previous report.[25,27] Briefly, the free amine containing intermediate *D* was synthesized from compound *C* based on the Hantzsch's thiazole condensation in ethanol at 80 °C. The compound *D* was reacted with 4-bromo-2-fluoro benzene sulfonyl chloride in pyridine solvent at room temperature for 5 h to produce the desired compound TBS. The detailed multi-step synthetic procedure and spectroscopic characterization of TBS are provided in the SI.

3.2 Drug loading in PAcVSA hydrogel

We used two different small molecule drugs for the present work. SDA is effective against a wide range of Gram-positive and Gram-negative bacteria, with a long history of use against various bacterial infections. The incorporation and release of SDA from a variety of delivery systems including polymer hydrogels has been reported.[42,43] TBS is a screened lead compound for antibacterial/antitumour purposes with good biocompatibility.[25–28] As described in the materials and methods section, 100 mg of dried PAcVSA hydrogel was immersed in 5 mg in of each SDA and TBS solution [prepared in 30 mL of ethanol : water (1 : 1)] at 37 °C, at pH 7 and shaken at 100 rpm. After 48 h of incubation, the hydrogel was carefully removed from the drug solution, washed with DI water, and dried in an oven at 60 °C for 48 h. The amount of the drug-loaded in PAcVSA hydrogel was calculated according to the original concentration of the drug molecules in solution and the concentration of the drugs in the solution after loading, which was quantified by UV-visible spectroscopy (JASCO V-750 spectrophotometer) *via* absorbance at wavelength 277 nm (SDA) and 304 nm (TBS), respectively as shown in Fig. 1a and b. As per calculation using a calibration plot, we found that SDA and TBS were loaded in PAcVSA hydrogel in 4.5 mg and 4.25 mg respectively.

The amount of drug loaded on hydrogel were calculated using eqn (7),

$$\text{Amount of drug loading} = (W_i - W_f) \quad (7)$$

where W_i is the initial amount of drug in solution before adsorption, and W_f is the amount of drug in solution after adsorption.

3.3 Characterization of pristine and small molecule loaded PAcVSA hydrogel

3.3.1 FTIR spectroscopy. For the FTIR analysis of pristine hydrogel, we dried the sample in the oven at 60 °C for 24 h and made powder using mortar-pestle. For drug-loaded hydrogel (PAcVSA_SDA and PAcVSA_TBS) we first loaded the drug into the PAcVSA hydrogel, and followed the same procedure as mentioned above. The FTIR spectra of synthesized PAcVSA hydrogel, SDA and TBS loaded PAcVSA hydrogels are shown in Fig. 2a. The FTIR spectra of the Ac and VSA monomers are shown in Fig. S2.

Comparison of the FTIR of PAcVSA with the Ac and VSA monomers reveals notable differences. The bands at 976 and 970 cm^{-1} observed for Ac and VSA monomers, respectively, are attributed to the vibration of –C=C–H in each monomer.[44] While the PAcVSA does not display a band in this region, the pronounced band at 1154 cm^{-1} is indicative of C–C stretching that arises because of the cross-linking between Ac and VSA monomers. Other characteristic FTIR bands for PAcVSA hydrogel were observed at 2969 cm^{-1} (–OH stretching of Ac), 1718 cm^{-1} (C=O stretching of Ac), 1156 cm^{-1} which is merged

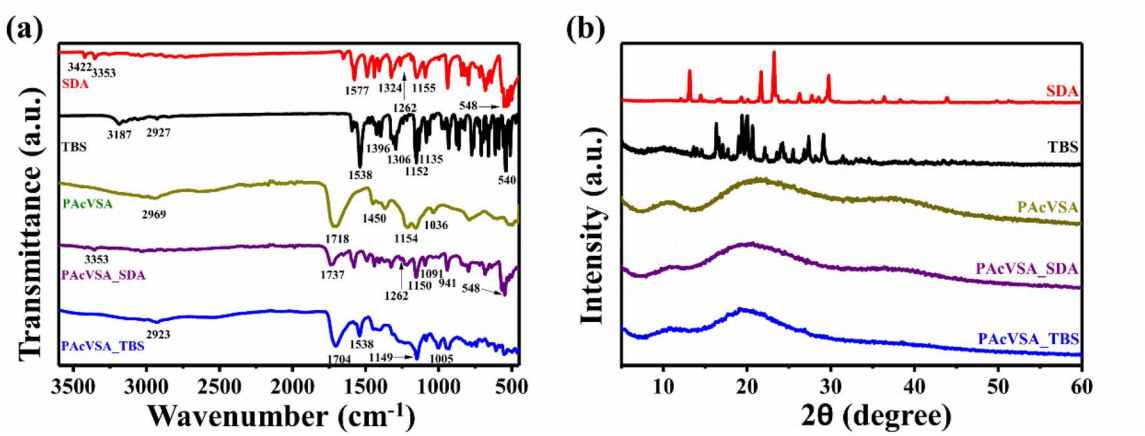

Fig. 2 (a) FT-IR spectra, and (b) PXRD spectra of SDA, TBS, PAcVSA, PAcVSA_SDA, PAcVSA_TBS.

with 1154 cm^{-1} and 1036 cm^{-1} due to SO_3^- and S=O vibrations of VSA, respectively.[16] For assessing the SDA and TBS-loaded PAcVSA hydrogels, FTIR spectra were recorded for bare SDA and TBS (Fig. 2a). The FTIR spectrum of SDA-loaded PAcVSA (PAcVSA_SDA) revealed shifting in band, with the SO_3^- group frequencies shifting from 1156 cm^{-1} and 1036 cm^{-1} to 1091 cm^{-1} and 941 cm^{-1}, respectively. Further, the sulfonamide stretching frequency of SDA shifted from 1155 cm^{-1} to 1150 cm^{-1} in the SDA-loaded hydrogel. The peak intensity for band at 1262 cm^{-1} was lower for the PAcVSA_SDA implying a possible weakening of the C=N bond stretching. Interestingly, the C=O stretching frequency of PAcVSA increased from 1718 cm^{-1} to 1737 cm^{-1} in PAcVSA_SDA which indicates the strengthening of the –C=O bond due to the sulfadiazine which has a strong electron-withdrawing effect.[45] While no new peaks were observed in the FTIR spectrum of PAcVSA_SDA, the shifting of several bands suggests weak forces of association between the hydrogel and the SDA. Further, for TBS, the band at 3187 cm^{-1} is attributed to –NH stretching of sulphonamide, while the band at 2927 cm^{-1} is attributed to =C–H stretching of aryl ring.[46] The band at 1538 cm^{-1} is related to C=C and C=N stretching vibration. Other notable FTIR peaks for TBS include the bands at 1396 cm^{-1}, 1306 cm^{-1}, and 1152 cm^{-1} arising from the SO_2 group, the 1135 cm^{-1} band attributed to C–F stretching and 540 cm^{-1} to C–Br stretching vibration.[27] The 1718 cm^{-1} peak of PAcVSA shifted to 1704 cm^{-1}, upon loading of the hydrogel with TBS, indicating an interaction of the C=O group of the hydrogel with the small molecule.[47,48] The intensity of the 1396 cm^{-1}, 1306 cm^{-1}, and 1152 cm^{-1} bands corresponding to the – SO_2^- group of TBS were significantly diminished in PAcVSA_TBS (TBS-loaded hydrogel) likely due to the hydrogen bonding between sulfonamide group of TBS molecules with a carboxylic acid group of PAcVSA hydrogel. The bands corresponding to SO_3^- of PAcVSA at 1156 cm^{-1} and 1036 cm^{-1}, were shifted to 1149 cm^{-1} and 1005 cm^{-1}, respectively, in PAcVSA_TBS, indicative of bonding interactions of the SO_3^- group with the TBS molecule. The lower intensity of NH vibrations in PAcVSA_TBS support their likely association with the –SO_2NH– of TBS. Notably, while no new peaks are observed in the FTIR spectrum of PAcVSA_TBS, the significant downward shifting of bands suggests the presence of soft forces including electrostatic interactions between the electronegative part of PAcVSA and the electropositive portion of TBS.[49]

3.3.2 Powder X-ray diffraction (PXRD). We performed powder X-ray diffraction (PXRD) on SDA, TBS, pristine PAcVSA, PAcVSA_SDA and PAcVSA_TBS, hydrogels for assessing changes in crystalline behaviour of the hydrogel upon loading of the small molecules. The PXRD results are shown in Fig. 2b. The PXRD of SDA showed sharp peaks at 2θ angles of 13.14°, 21.69°, 23.24° and 29.74°, indicating the crystalline nature of SDA. Similarly, the crystalline character of TBS was indicated by the presence of strong sharp peaks at 2θ angles of 16.34°, 19.40°, 20°, 20.66°, 24.23°, 27.35°, and 29.12°. The PXRD of pristine PAcVSA hydrogel showed a broad peak at 2θ angle of 21.42° and a broad shoulder peak at 37.47°, implying amorphous nature of the hydrogel. The PXRD of drug loaded hydrogels *i.e.*, PAcVSA_SDA and PAcVSA_TBS displayed broad peaks at 2θ angles of 19.10°, 37.51° and 20.12°, 37.19°, respectively, which are closer to the pristine PAcVSA hydrogel. The small differences in PXRD of the loaded *versus* unloaded PAcVSA can be attributed to the loading of only a small equivalent of the molecules (SDA and TBS) compared to the proportion of functional groups of the hydrogel.[47,50] The absence of new peaks in the XRD of the small molecule-loaded hydrogels suggest dispersion of the cargo in the polymeric matrix without disruption of the chemical scaffold of the hydrogel.[50]

3.3.3 Thermogravimetric analysis (TGA). We next investigated the thermal stability of the small molecule loaded hydrogels *via* thermogravimetric analysis (TGA). The TGA of PAcVSA_SDA, PAcVSA_TBS SDA, TBS and pristine PAcVSA hydrogel are shown in Fig. 3.

The TGA of pristine and drug-loaded hydrogels indicate degradation in two stages. The pristine PAcVSA hydrogel is sufficiently stable up to 185 °C. By this temperature, 8% weight loss was observed for the pristine hydrogel which is attributed to the loss of water. The next weight loss for the pristine PAcVSA of up to 24% was observed between 185 °C to 310 °C while the maximum weight loss of 47% was observed from 310 °C to 500 °C. In comparison, the performance of PAcVSA_SDA was stable up to 5% weight loss up to 185 °C, followed by 22% between 185 °C to 310 °C and a maximum loss of 38% between 310 °C to 500 °C. And the PAcVSA_TBS hydrogel was stable up to 185 °C with 10% weight loss, followed by 19% between 185 °C to 310 °C and subsequently to 46% between 310 °C to 500 °C. At 500 °C, the PAcVSA_SDA and PAcVSA_TBS hydrogels degraded by 65% and 74%, respectively, compared to nearly 79% degradation observed for pristine PAcVSA. The improvement in thermal stability is approximately 14% and 5% for PAcVSA_SDA and PAcVSA_TBS, respectively.[51,52] The greater thermal stability of PAcVSA_SDA and PAcVSA_TBS hydrogels can be attributed to the (1) good thermal stability of SDA and TBS, and (2) favourable forces of interaction between the polymer matrix and the small molecules that limit the molecular chain movement of the polymer. The improved thermal stability of the small molecules loaded PAcVSA hydrogel bodes well for their further consideration and scrutiny as drug release agents.

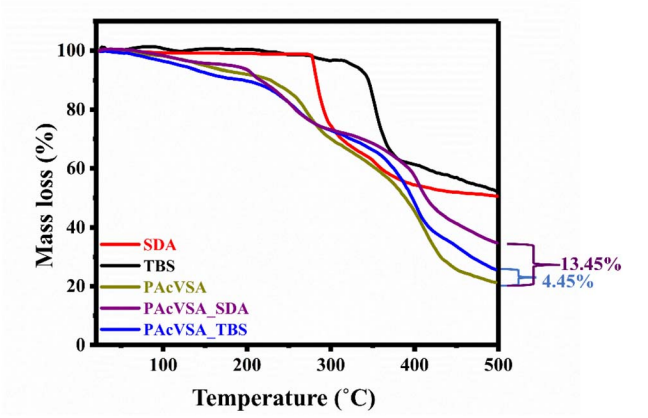

Fig. 3 Thermogravimetric analysis of SDA, TBS, PAcVSA, PAcVSA_SDA and PAcVSA_TBS.

3.3.4 Field emission-scanning electron microscopy (FESEM). The morphology of pristine and small molecule loaded hydrogel was assessed by field emission scanning electron microscopy (FESEM). FESEM analysis samples were first swollen in pH 7 buffer and then lyophilized. As shown in Fig. 4a, pristine PAcVSA hydrogel displays a porous morphology and Fig. 4b shows the magnified image of pristine PAcVSA hydrogel which shows smooth edges. Interestingly, the SDA loaded hydrogel displays substantive disruption in the porous structure of the hydrogel. The collapsed and closely packed morphology of PAcVSA_SDA is visible in Fig. 4c, and the zoomed image of PAcVSA_SDA (Fig. 4d) indicates locations that show SDA loading on hydrogel. The morphology of PAcVSA_TBS hydrogel retains the porous character albeit with irregular or rough edges as shown in Fig. 4e. The distortion in porosity and the collapsed architecture of PAcVSA_TBS are evident in the magnified section shown in Fig. 4f. EDX shows that both TBS and SDA was loaded on the PAcVSA hydrogel as PAcVSA hydrogel shows only C, O and S, while after loading of TBS and SDA EDX mapping shows the C, O, N, and S elements (Fig. S3). Overall, the dispersion of SDA and TBS into the hydrogel matrix creates disruptions in the regular porous architecture of PAcVSA.[53,54]

3.3.5 Rheology of pristine and small molecule loaded PAcVSA. We next investigated the dynamic rheological characteristics of the pristine PAcVSA and of PAcVSA_SDA and PAcVSA_TBS. Oscillatory strain sweeps were performed at 25 °C to identify the linear viscoelastic region (LVR) of the hydrogel. The storage (G') and loss (G'') moduli of the pristine PAcVSA, PAcVSA_SDA, and PAcVSA_TBS hydrogel intersected at critical strain values of 30%, 60%, and 42.4%, respectively (Fig. 5a and b). The higher critical strain necessary for transitioning PAcVSA_SDA and PAcVSA_TBS to a fluidic state compared to pristine PAcVSA highlights the ability of the small molecule loaded hydrogels to maintain their structural integrity and resist deformation. The higher crossover points of G' and G'' of

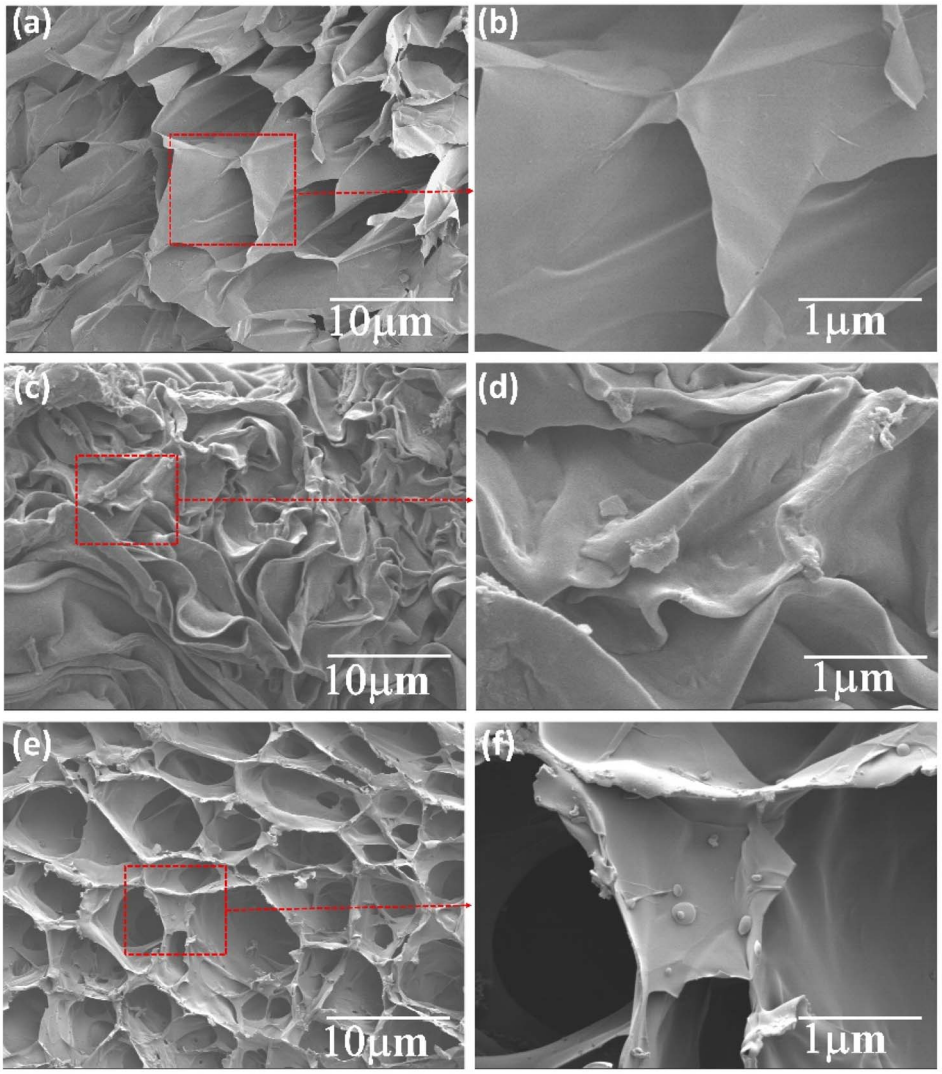

Fig. 4 SEM images of (a) PAcVSA, (b) magnified image of a, (c) PAcVSA_SDA, (d) magnified image of (c) (red box) showing SDA loading, (e) PAcVSA_TBS, and (f) magnified image of (e) (red box) showing TBS loading.

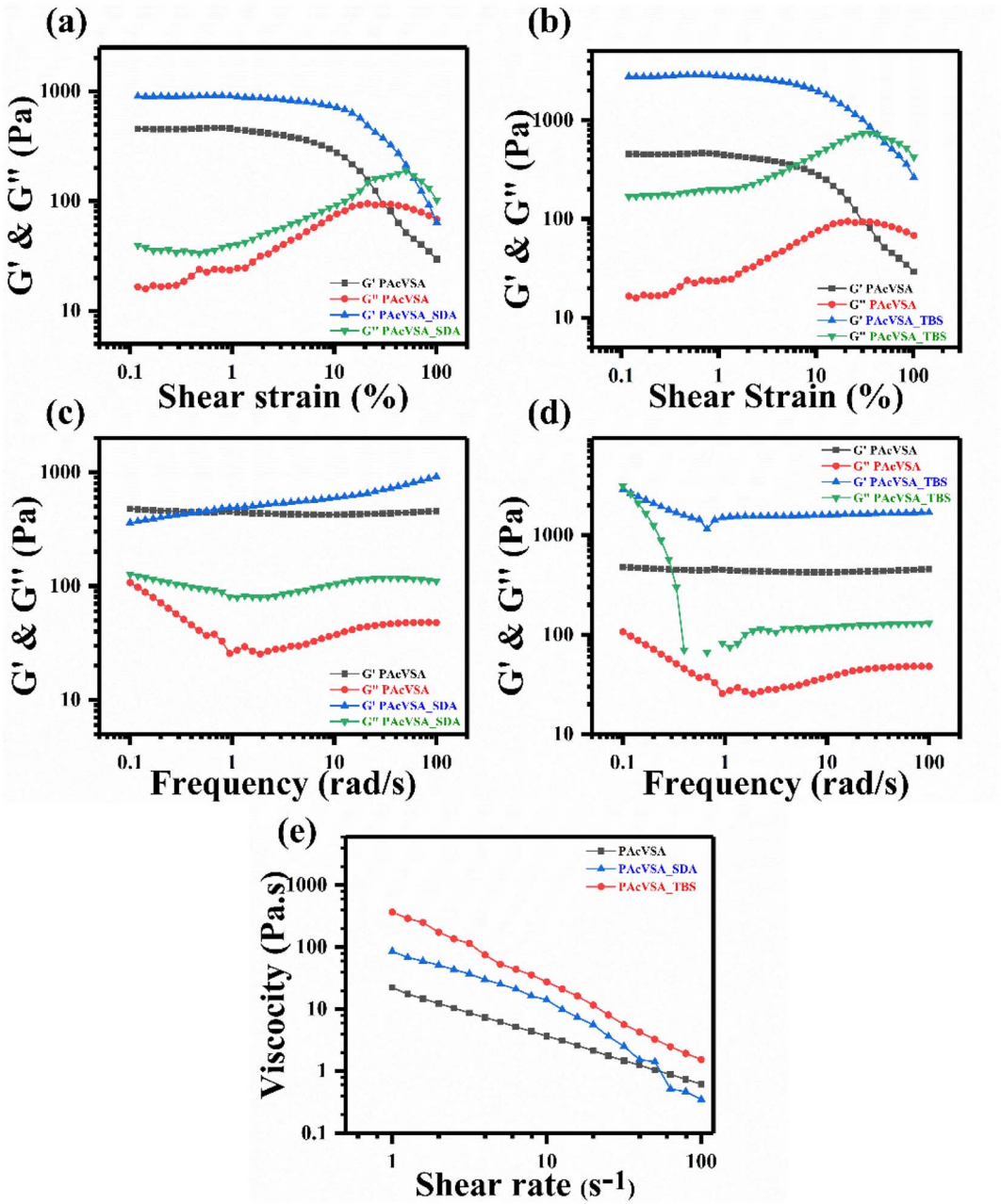

Fig. 5 Rheological properties of PAcVSA, PAcVSA_SDA and PAcVSA_TBS hydrogels. (a) and (b) compare the Storage (G') and Loss (G'') modulus of PAcVSA, PAcVSA_SDA and PAcVSA_TBS hydrogel with respect to shear strain, respectively, (c) and (d) compare the Storage (G') and loss (G'') modulus of PAcVSA, PAcVSA_SDA and PAcVSA_TBS hydrogel with respect to frequency sweep, respectively, (e) shows the shear thinning behaviour of PAcVSA, PAcVSA_SDA and PAcVSA_TBS hydrogel.

PAcVSA_SDA and PAcVSA_TBS are likely to contribute to the gradual release of the loaded small molecules.[55,56]

The mechanical strength of PAcVSA was evaluated by conducting frequency sweep measurements within the LVR with and without loading of TBS and SDA into the hydrogel. As shown in Fig. 5c and d, the G' was higher than the G'' for the pristine PAcVSA, PAcVSA_SDA and PAcVSA_TBS, implying greater gel-like character for all the hydrogels. The increase of G' and G'' values of PAcVSA_SDA and PAcVSA_TBS as compared to pristine PAcVSA reflects the loading of the small molecules into the polymeric matrix.[56] The introduction of small molecules enhances the hydrogel's cross-linking density through interactions such as hydrogen bonding, ionic interactions, or *via* hydrophobic effects. These interactions likely result in a stiffer, more elastic material with increased G' values (elasticity) and G'' values (energy dissipation), reflecting improved structural integrity and mechanical strength.[57–59] A comparison of the shear-thinning behaviour of pristine and small molecule loaded hydrogels at 25 °C suggests an interesting similarity in the performance of PAcVSA, PAcVSA_SDA and PAcVSA_TBS

(Fig. 5e). The shear thinning displayed a nearly linear reduction in shear thinning with the increase in shear rate throughout.[56] The addition of small molecules increases the hydrogel's viscosity and enhances its viscoelastic behaviour, as indicated by higher G' and G'' values. This suggests increased internal friction and a higher damping factor ($\tan\delta$), leading to more complex flow behaviour under stress.[60,61] As with increasing the shear rate the cross-linked polymeric network structure starts to disrupt.[62]

3.4 pH-sensitive swelling study of hydrogel

During synthesis of the PAcVSA hydrogel the change in initiator from BPO to APS for reducing the timing of gelation may affect the swelling capacity of the hydrogel in media of different pH. Accordingly, to investigate the swelling behaviour of synthetically modified PAcVSA hydrogel, we first studied the swelling of the hydrogel at pH 5, 7.4 and 8. These pH were chosen for the study since pH $\approx$ 5 corresponds to the tumor microenvironment, and pH $\approx$ 8 corresponds to the intestinal or blood environment. The range covers typical physiological scenarios. The gravimetric method was used to determine the Percentage swelling ratio (SR (%)) of PAcVSA hydrogel as per eqn (8).[63,64]

$$\text{SR} \quad (\%) = \frac{(W_s - W_d)}{W_d} \times 100 \qquad (8)$$

where W_s is the hydrogel weight in a swollen state (g) and W_d is the weight of dry hydrogel (g).

Comparison of the swelling ratio at pH 5, 7.4 and 8 (Fig. 6a) indicate the lowest overall swelling ratio of the hydrogel at pH 5.

As shown in Fig. 6b, the swelling ratio of PAcVSA displayed a rapid increase initially before attaining a constant proportion. In contrast to pH 5, the hydrogel swelling ratio displayed a remarkable increase at pH 7.4 especially over the first 12 h, before reaching equilibration at ~80 h. The pH-sensitive behaviour of PAcVSA is exemplified by the higher swelling ratio at pH 8 compared to pH 7.4. A substantially greater swelling ratio was observed for PAcVSA at pH 8 compared to pH 7.4 after the first 12 h, emphasizing the pH-sensitive character of the hydrogel. The swelling ratio continued to increase for the hydrogel at pH 8 till 96 h, albeit at a diminished rate. The greater SR(%) of PAcVSA at pH 8 compared to pH 5 and 7.4, can be correlated to protonation or deprotonation of the constituent functional groups occurring at each pH. Since the pK_a of the carboxylic acid of polyacrylic acid is 4.5 and for sulfonate of vinyl sulfonic acid is −1.3, at pH 5 some of the COO^- gets protonated while the SO_3^- is in anionic form.[65,66] The protonation of these groups likely facilitates hydrogen bonding between them, resulting in intra-polymer interactions gaining prominence compared to polymer–water interactions, and increasing the propensity of the polymer to contract. Strong intra-polymer interactions would mitigate electrostatic repulsion between residual numbers of charged functional groups, further constraining the ability of the polymeric network to swell. At pH 7.4, a significant proportion of the COO^- and SO_3^- groups are deprotonated resulting in the disruption of intra-polymer hydrogen bonding. The increased electrostatic repulsion between the carboxylate and sulfonic anions likely facilitates greater relaxation of the polymer network.[67,68] A small

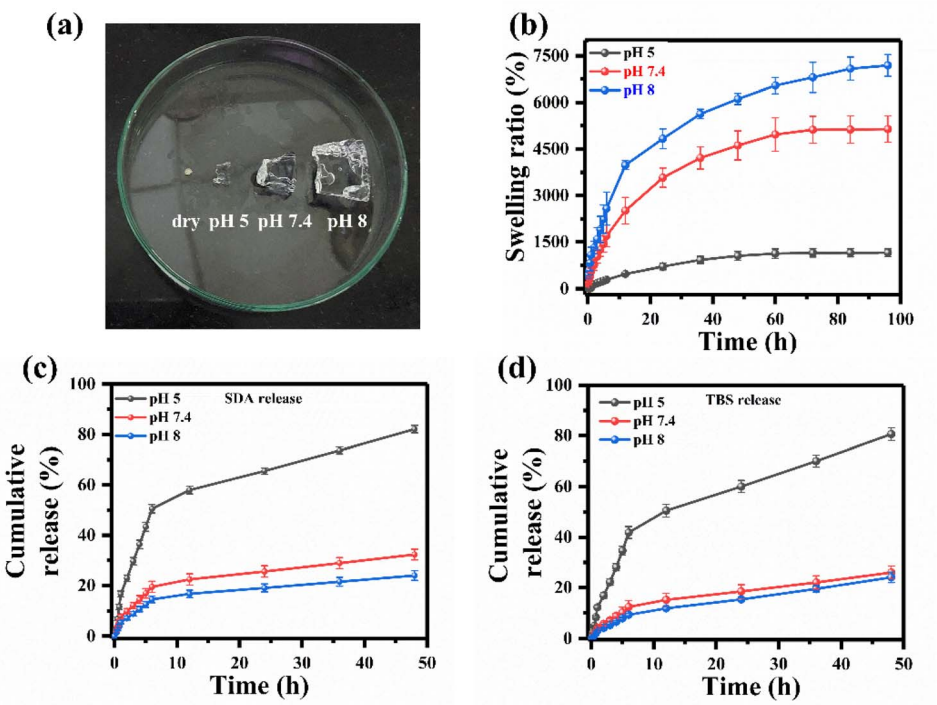

Fig. 6 (a) Photograph of swelling behaviour, (b) change in swelling ratio (%) over time for PAcVSA hydrogels in different pH buffers (pH 5, pH 7.4, and pH 8), (c) and (d) the cumulative release percentage over time of SDA and TBS from the PAcVSA_SDA and PAcVSA_TBS hydrogel matrix, respectively.

Table 1 Modelling parameters of the kinetics of small molecule release from PAcVSA_TBS and PAcVSA_SDA estimated from Korsmeyer–Peppas and Higuchi models

		Hydrogel samples						
			PAcVSA_SDA			PAcVSA_TBS		
Kinetic models	Parameters	pH	5	7.4	8	5	7.4	8
Korsmeyer–Peppas	R^2		0.95083	0.96502	0.96265	0.97106	0.98392	0.99181
	k (h^{-1})		19.8518	8.23852	6.00869	14.76027	4.54689	3.12805
	n		0.37894	0.36216	0.36754	0.44498	0.45047	0.52047
Higuchi	R^2		0.89977	0.89346	0.89811	0.96294	0.97762	0.99096
	k (h^{-1})		27.27353	10.75832	7.97509	24.85281	7.80002	6.67424

increase in pH from 7.4 to 8 results in substantive ionization of carboxylate and sulfonic anions resulting in further disruption of intra-polymer hydrogen bonding and enhancing the swelling propensity of the hydrogel.[69] The PAcVSA hydrogel exhibits a significant increase in swelling behaviour (in terms of SR(%)) when the pH value exceeds 7.4. The present results indicate that changing the pH value from 5 to 8 leads to a substantial variation in swelling ratio (%), reaching approximately 6000% or more, as illustrated in Fig. 6b. The lower swelling profile observed for the PAcVSA synthesized in the present work compared to previously reported formulation may be attributed to use of a different initiator during synthesis.[16] Nevertheless, the swelling behaviour displayed by the PAcVSA hydrogels is superior to that reported for other pH-sensitive acrylic acid containing hydrogels. For instance, the poly(acrylamide-*co*-acrylic acid) hydrogel used for the controlled release of gentamicin sulphate shows a swelling variation of 730% from pH 4.5 to pH 7.[23] Likewise, the poly(acrylamide-*co*-acrylic acid)/chitosan semi IPN hydrogel, studied for the release behaviour of ranitidine hydrochloride, exhibits a swelling variation of 1174% from pH 2 to pH 10.[70] The dramatic transition in swelling behaviour of PAcVSA reported here in response to relatively small pH changes is likely to encourage distinctive small molecule release profiles.

3.5 *In vitro* release of SDA and TBS from loaded PAcVSA

The *in vitro* release of SDA and TBS from PAcVSA_SDA and PAcVSA_TBS, respectively, were studied at pH 5, 7.4 and 8. As illustrated in Fig. 6c and d, the release of SDA and TBS are pH dependent, and the release rate increased markedly as the pH decreased from 8 to 5. At pH 8, the PAcVSA_SDA and PAcVSA_TBS hydrogels released only 5.4% and 3.2% of the drug molecules, respectively, in the first 1 h and ~20% after 24 h. In, neutral conditions (pH 7.4), the hydrogels show 7.6% of SDA and 4.2% of TBS initially in first 1 h and ~30% (SDA) and ~25% (TBS) after 24 h. In contrast, exposure of the loaded hydrogels to pH 5 resulted in the release of 16.6% SDA and 12.2% TBS after 1 h. The released quantities reached 82.1% for SDA and 80.6% of TBS after 24 h, which is about six times higher than that of pH 8 and five times higher than pH 7.4. The observed release profile can be justified based on weaker electrostatic interaction at pH 5 between the hydrogel and small molecules due to protonation of carboxylate groups in the former.[71] In addition, the greater hydrophilicity and solubility of SDA and TBS due to protonated sulfonamide groups at the acidic pH likely contribute to their faster release.[71] Progressively stronger electrostatic interactions at pH 7.4 and pH 8 between the positively charged amine groups of SDA and TBS with negatively charged carboxyl groups, blocks the release of the small molecules from the hydrogel. The release profiles of SDA and TBS from PAcVSA are compared with other prominent pH responsive hydrogels later in this article.

The quantitative modelling of kinetics of small molecule release from PAcVSA_SDA and PAcVSA_TBS is likely to shed light on the mechanism of diffusion in each case.[72] The accurate quantitative modelling of experimentally observed drug release is a key indicator of the predictability of hydrogel behaviour. We modelled the time-resolved cumulative release percentage using five different models namely zero-order, first-order, Higuchi, Korsmeyer–Peppas (KP) and Hixson–Crowell.[72–74] These models were applied on both PAcVSA_SDA and PAcVSA_TBS for release over 48 h in medium of pH solutions 5, 7.4 and 8. The model with the values of coefficient of regression (R^2) closest to 1 indicates the best fit to experimental data. The KP and Higuchi models delivered the best R^2 for the release of SDA and TBS across all three pH being tested. Table 1 lists the calculated parameters for these two models applied on PAcVSA_SDA and PAcVSA_TBS. The release behaviour of both the small molecules are best fit by KP model (Fig. 7a and b). While the Higuchi model fit the release of PAcVSA_TBS well, it was less effective for modelling the release of PAcVSA_SDA (Fig. 7c and d). The results of fitting zero-order, first-order and Hixson–Crowell models are provided in SI (Fig. S4 and Table S1).

The KP model offers a straightforward empirical approach for describing release of small molecules from hydrogels.[75] In addition to the payload release rate, the KP model provides a release exponent 'n,' that can define the broad contours of underlying release mechanism. In particular, the release of drugs from swellable carrier is driven by Fickian diffusion when the value of $n \leq 0.43$. If 'n' lies in the range, $0.43 < n < 0.85$, the release of the drug is controlled by diffusion and polymer relaxation (non-Fickian or anomalous transport). Also, if $n > 0.85$, the release is controlled by "super case II transport".[37] Interestingly, the release exponent 'n' for SDA release from PAcVSA_SDA is $\leq$0.43 implying that the release of SDA from the hydrogel follows Fickian diffusion (Table 1). In contrast, for

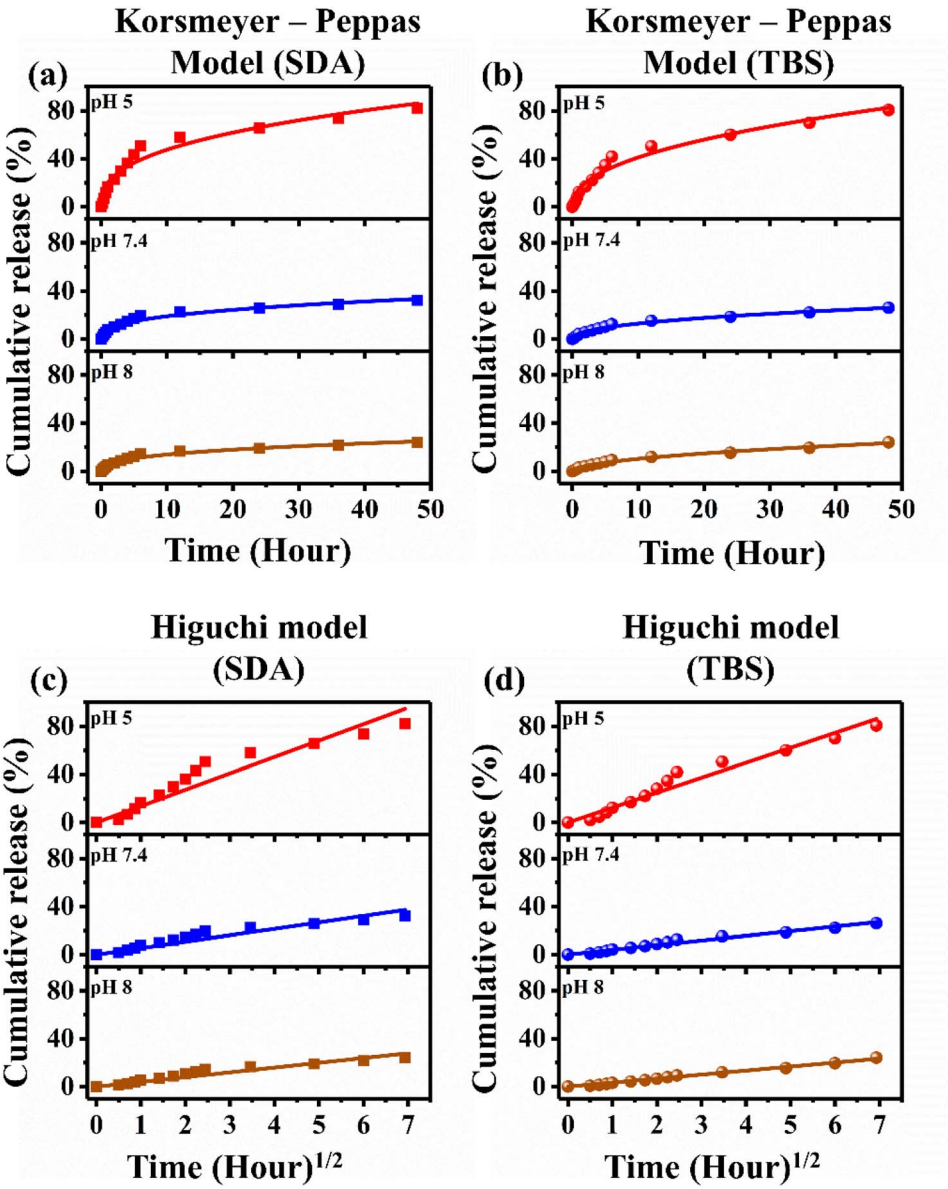

Fig. 7 Comparison of modelling of the kinetics of release of SDA and TBS from PAcVSA. (a) and (b) Show Korsmeyer–Peppas fitting for SDA and TBS release from PAcVSA_SDA and PAcVSA in pH 5, 7.4, and 8 buffer media, respectively. (c), and (d) Show Higuchi fitting for SDA and TBS release from PAcVSA_SDA and PAcVSA_TBS hydrogel in pH 5, 7.4, and 8 buffer media, respectively.

PAcVSA_TBS the release exponent n lies in the range of $0.43 < n < 0.85$ suggesting that TBS release from the hydrogel is controlled by non-Fickian diffusion or due to the polymer relaxation in pH 5, 7.4 and 8 (Table 1). The comparable values of n for PAcVSA_SDA across pH 5, 7.4 and 8, are instructive as they suggest a similar extent of diffusion-driven release of SDA from the hydrogel despite dramatic changes in the intra-polymer interactions that have been outlined in the previous section. On the other hand, the value of n for PAcVSA_TBS gradually increases from pH 5 to 7.4 and 8, reflecting the effect of greater relaxation of the polymer network due to deprotonation of the constituent COO^- and SO_3^- groups. The movement of small molecules from poly(acrylic acid) containing composite hydrogels has been previously justified based on changes in pore sizes of the hydrogel upon change in pH of the surrounding medium.[23] Polymer relaxation is the principal mechanism for release of small molecules from hydrogels with strong cross-linking, inter-penetrating network architecture, or bearing magnetic nanoparticles.[24,76] Considering that Fickian diffusion is responsible for the release of SDA irrespective of pH, the changes in pore sizes clearly do not impact the mobility of the drug. TBS is a larger molecule compared to SDA and relies mainly on polymer-chain relaxation to affect its release from the hydrogel. The present observation of dissimilar mechanisms governing two different small molecules from the same hydrogel is quite unique. The KP model is constrained by inability to robustly characterize long-term limit of the release kinetics beyond approximately 60% of the released material.

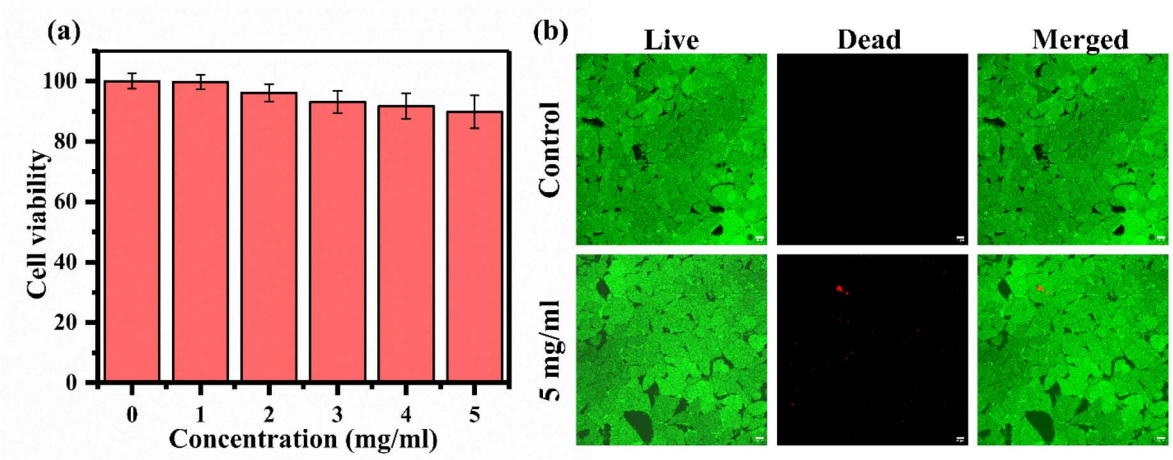

Fig. 8 (a) MTT assay for PAcVSA hydrogel, and (b) live/dead cell assay performed on HEK 293T cells incubated with PAcVSA hydrogel.

Nevertheless, the difference in overall rate of release of SDA and TBS from the cognate loaded hydrogels is best captured by the KP model. At pH 5, the rate of release of SDA from PAcVSA_SDA was 19.85 h^{-1} while the rate of release of TBS from PAcVSA_TBS was 14.76 h^{-1}. The greater release of SDA is evident from the cumulative release percentage profile (Fig. 6c and d). While the application of the Higuchi model on release of TBS results in

Table 2 Comparison of small molecule release behaviour of pH-responsive hydrogels

No.	Polymer composition	Drug loaded	pH of release buffer medium	Release time (H)	% Release
1	PLGA polymeric nanoparticles[78]	Mometasone furoate	Cryoprotection in sucrose pH 6.4	180	87
			Cryoprotection in sucrose pH 7.4		55
			Cryoprotection in mannitol pH 6.4		70
			Cryoprotection in mannitol pH 7.4		60
2	GG-GA-La-GO[79]	Amoxicillin trihydrate	pH 7.4	6.5	60
3	DOX-CaCO3-alginate[80]	Doxorubicin	pH 4.5	48	56
			pH 6.5		30
			pH 7.4		6
4	Cs/HA/Fe_3O_4 (ref. 39)	Ciprofloxacin	pH 7.4	13	Nearly 100
			pH 8		
			pH 5		
			pH 2		
5	Su-CNC/PNIPAm[5]	Famotidine	pH 2	2	100
			pH 10	8	100
6	CA-DA/OP6 (ref. 81)	Doxorubicin	pH 5.7	60	87
			pH 6.8		75
			pH 7.4		52
7	Chito/HA[82]	Ciprofloxacin	pH 5.5	6	78.8
			pH 7.4		86.1
		Curcumin	pH 5.5		48.7
			pH 7.4		89.9
8	CP-g-AMPS[83]	Ellagic acid		48	
	KAE-6		pH 1.2		92.13
			pH 7.4		77.28
	KAE-3		pH 1.2		57.03
			pH 7.4		46
9	H1 PAM[84]	Dependal-M	pH 5.8	1.5	16.8
	H1 PAM				16.4
10	PAcVSA[a]	Sulfadiazine	pH 5	48	82.12
			pH 7.4		32.35
			pH 8		24
		TBS	pH 5		80.67
			pH 7.4		26
			pH 8		24.09

[a] Current work.

a rate of release of 24.8 h^{-1}, the fitting of SDA release is not satisfactory and is therefore unsuitable for comparison.

3.6 Cytotoxicity of PAcVSA hydrogel

We wanted to assess cytotoxicity of the PAcVSA prepared in the present work, considering the changes in procedure of preparation deployed compared to previous reports. To investigate the cytotoxicity we used 1 to 5 mg mL^{-1} concentration of hydrogel as reported previously.[16]

We performed MTT and live/dead cell assay to evaluate the cytotoxicity of PAcVSA towards HEK 293T cells.[40,41] As shown in Fig. 8a, the PAcVSA hydrogel is not toxic to HEK 293T cells between 1 to 5 mg mL^{-1} for 72 h. The live/dead assay was performed using calcein AM dye (green) for live cell staining and propidium iodide dye (red) for dead cell staining. Calcein AM is rapidly hydrolyzed by cellular esterase within live cells, resulting in the cleavage of the AM group. This hydrolysis converts the non-fluorescent Calcein AM into a strongly green fluorescent Calcein. In contrast, Propidium Iodide (PI) can only traverse compromised cell membranes and intercalates with DNA and RNA within dead cells, thereby emitting red fluorescence.[77] Non-treated HEK 293T cells were used as a control. HEK 293T cells were treated with different concentrations of the PAcVSA hydrogel ranging from 1 to 5 mg mL^{-1}. The treatment of HEK 293T cells with PAcVSA at 5 mg mL^{-1} did not result in any cell death (Fig. 8b and S5) for up to 72 h. Overall, these results suggest the biocompatibility of the PAcVSA hydrogel making it an attractive carrier for pharmaceutical agents.

3.7 Comparison of PAcVSA with reported pH-responsive hydrogel carriers

We performed an extensive literature study on small molecule/drug release profiles from pH-responsive hydrogels. Our survey is listed in Table 2. Two aspects emerge from a scrutiny of performance of the different pH-responsive carriers. Firstly, the PAcVSA hydrogel described in this work exhibits remarkable release profile in mildly acidic conditions (pH 5). Secondly, the hydrogel described in this work displays the greatest differential in small molecule release between pH 5 and 8. The release of 82.1% SDA and 80.6% TBS in a strongly pH-dependent manner over a prolonged duration of time without use of any other adjuvants highlights the distinctive of the PAcVSA hydrogel. Nearly all the previously reported hydrogels listed in Table 2 have been characterized by the Korsmeyer–Peppas model. In this regard, PAcVSA is unique for eliciting different mechanisms for two different small molecule cargo; polymer relaxation for release of TBS, and Fickian diffusion for release of SDA. This unique behaviour of PAcVSA is rarely reported in recent hydrogel literature, and indicates the singular interactions that are exerted by the polymeric scaffold and suggest versatility of use.

4. Conclusion

In this work, we have repurposed a pH-sensitive PAcVSA hydrogel that has been previously reported for adsorptive remediation of organic dye.[16] Subtle modifications in the synthesis of the PAcVSA used in this work enable a distinctive combination of adhesion and release of two different small molecules. Accordingly, the synthesized PAcVSA hydrogel displays an excellent swelling ratio of 6000% or more, and a remarkable release of the loaded small molecules at modest acidic pH of 5. The difference in cumulative release percentage of both small molecules from the cognate loaded hydrogels between pH 5 and 8 is superlative in comparison to previously reported pH-responsive hydrogel carriers. The two molecules used in this work represent an established pharmaceutical agent (SDA) and a molecule (TBS) with promising drug-like behaviour.[25] The pH-sensitive modulation of charged groups in the hydrogel is accompanied by different mechanisms of release of the small molecules, namely Fickian diffusion for SDA and by non-Fickian diffusion or due to the polymer relaxation for TBS. Our PAcVSA hydrogel is novel considering the sparse reports of hydrogels displaying variability in mechanism of release for different cargo.[73]

The cross-use of synthetic hydrogels between adsorption of environmentally relevant analytes and release of small molecule pharmaceuticals is extremely rare. While such cross-use of biopolymer composite hydrogels in environmental mitigation and for drug release has been reported in slightly greater numbers, the performance of the hydrogels is rarely benchmarked against the best-in-class synthetic or composite hydrogel candidates. Thus, the question about whether a specific synthetic hydrogel that has been developed and demonstrated for environmental applications can also be readily used for loading and release of small molecule drugs is yet to be convincingly addressed. The strength of the present work lies in the unambiguous demonstration of PAcVSA as a robust and superlative pH-responsive delivery agent of small molecules, based on subtle modifications in its formulation that has been previously reported as an attractive adsorbent of environmentally relevant cationic dyes. Further, studies on small molecule release by hydrogels are predominantly focused on established pharmaceutical agents. The applicability of a hydrogel for the carry and release of small molecules that may be related to but distinct from a known drug is rarely addressed. In this context, the ability of PAcVSA to carry and release SDA and TBS highlights the capability of the hydrogel and sheds light on interesting differences in the mechanism of their release. This study introduces the paradigm of assessing multiple small molecule drugs on the same hydrogel, and is thus significant in the broader context of hydrogel research. The present study is limited by its inability to comment on the efficacy of the released small molecule drugs. Notwithstanding the responsive behaviour of the PAcVSA hydrogel towards physiologically relevant pH range of fluid environments, the ability of specific pharmaceutical agents to exert their activity post-release remains to be experimentally investigated. Similarly, considering the design of the present work, the compatibility of PAcVSA with various chemical scaffolds underlying drug development cannot simply be extrapolated and would require thorough experimentation.

The application of synthesized materials for diverse and disconnected functions is an accepted milestone of sustainable

design. There are very few reports of intentional repurposing of synthetic hydrogels across the two domains, and this work successfully demonstrates the same. Questions surrounding additional tunability of such cross-use hydrogels, and assessment of the pharmacological efficacy of released drugs, are likely to improve their potential for real deployment, and are being investigated in our laboratory.

Conflicts of interest

There are no conflicts of interest to declare.

Data availability

All data supporting this article are included in the main text and SI.

Acknowledgements

The authors are grateful to Central Instrumental Facility (CIF) of IIT Gandhinagar for their support towards this work. B. D. gratefully acknowledges financial support for this work by GUJCOST vide project no. GUJCOST/STI/2023-24/254. R. S. is grateful to IIT Gandhinagar for a post-doctoral fellowship.

References

1 M. Song, J. Wang, J. He, D. Kan, K. Chen and J. Lu, Synthesis of hydrogels and their progress in environmental remediation and antimicrobial application, *Gels*, 2023, **9**, 16, DOI: 10.3390/GELS9010016.

2 N. H. Thang, T. B. Chien and D. X. Cuong, Polymer-based hydrogels applied in drug delivery: an overview, *Gels*, 2023, **9**, 523, DOI: 10.3390/GELS9070523.

3 M. Ahmaruzzaman, *et al.*, Polymeric hydrogels-based materials for wastewater treatment, *Chemosphere*, 2023, **331**, 138743, DOI: 10.1016/J.CHEMOSPHERE.2023.138743.

4 Z. Han, *et al.*, Dual pH-responsive hydrogel actuator for lipophilic drug delivery, *ACS Appl. Mater. Interfaces*, 2020, **12**(10), 12010–12017, DOI: 10.1021/acsami.9b21713.

5 H. E. Emam and T. I. Shaheen, Design of a dual pH and temperature responsive hydrogel based on esterified cellulose nanocrystals for potential drug release, *Carbohydr. Polym.*, 2022, **278**, 118925, DOI: 10.1016/j.carbpol.2021.118925.

6 Y. Leng, *et al.*, Stimuli-responsive phosphate hydrogel: a study on swelling behavior, mechanical properties, and application in expansion microscopy, *ACS Omega*, 2024, **9**(36), 37687–37701, DOI: 10.1021/ACSOMEGA.4C02475/ASSET/IMAGES/LARGE/AO4C02475_0012.JPEG.

7 I. S. Protsak and Y. M. Morozov, Fundamentals and advances in stimuli-responsive hydrogels and their applications: a review, *Gels*, 2025, **11**(1), 30, DOI: 10.3390/GELS11010030.

8 A. Nuthanakanti and S. G. Srivatsan, Multi-stimuli responsive heterotypic hydrogels based on nucleolipids show selective dye adsorption, *Nanoscale Adv.*, 2020, **2**(9), 4161–4171, DOI: 10.1039/d0na00509f.

9 Y. H. An, *et al.*, Facilitated transdermal drug delivery using nanocarriers-embedded electroconductive hydrogel coupled with reverse electrodialysis-driven iontophoresis, *ACS Nano*, 2020, **14**(4), 4523–4535, DOI: 10.1021/acsnano.0c00007.

10 S. Chen, *et al.*, Smart microneedle fabricated with silk fibroin combined semi-interpenetrating network hydrogel for glucose-responsive insulin delivery, *ACS Biomater. Sci. Eng.*, 2019, **5**(11), 5781–5789, DOI: 10.1021/acsbiomaterials.9b00532.

11 J. C. Q. de Stéfano, V. Abundis-Correa, S. D. Herrera-Flores and A. J. Alvarez, PH-sensitive starch-based hydrogels: synthesis and effect of molecular components on drug release behavior, *Polymers*, 2020, **12**(9), 1–14, DOI: 10.3390/polym12091974.

12 M. Vázquez-González and I. Willner, Stimuli-responsive biomolecule-based hydrogels and their applications, *Angew. Chem., Int. Ed.*, 2020, **59**(36), 15342–15377, DOI: 10.1002/anie.201907670.

13 R. Singh and B. Datta, Advances in biomedical and environmental applications of magnetic hydrogels, *ACS Appl. Polym. Mater.*, 2023, **5**(7), 5474–5494, DOI: 10.1021/acsapm.3c00815.

14 A. L. Chau, P. T. Getty, A. R. Rhode, C. M. Bates, C. J. Hawker and A. A. Pitenis, Superlubricity of pH-responsive hydrogels in extreme environments, *Front. Chem.*, 2022, **10**, 891519, DOI: 10.3389/FCHEM.2022.891519/BIBTEX.

15 B. Singh and Rohit, Tailoring and evaluating poly(vinyl sulfonic acid)-sterculia gum network hydrogel for biomedical applications, *Materialia*, 2022, **25**, 101524, DOI: 10.1016/J.MTLA.2022.101524.

16 R. Singh, D. Pal, A. Mathur, A. Singh, M. A. Krishnan and S. Chattopadhyay, An efficient pH sensitive hydrogel, with biocompatibility and high reusability for removal of methylene blue dye from aqueous solution, *React. Funct. Polym.*, 2019, **144**, 104346, DOI: 10.1016/j.reactfunctpolym.2019.104346.

17 H. Arkaban, M. Barani, M. R. Akbarizadeh, N. Pal Singh Chauhan, S. Jadoun, M. Dehghani Soltani and P. Zarrintaj, Polyacrylic acid nanoplatforms: antimicrobial, tissue engineering, and cancer theranostic applications, *Polymers*, 2022, **14**(6), 1259, DOI: 10.3390/polym14061259.

18 G. Ujwala, C. Madhavi, O. S. Reddy, R. R. Raju, T. M. Kalyankar and K. Anitha, Development and characterization of sodium alginate-g-poly(acrylic acid-co-2-acrylamido-2-methyl-1-propane sulfonic acid)/locust bean gum microbeads containing nickel ferrite nanoparticles for pH-responsive release of doxorubicin, *Mater. Today Proc.*, 2023, **92**, 899–905, DOI: 10.1016/J.MATPR.2023.04.482.

19 Y. Chen, X. Guo, A. Mensah, Q. Wang and Q. Wei, Nature-inspired hydrogel network for efficient tissue-specific underwater adhesive, *ACS Appl. Mater. Interfaces*, 2021, **13**(50), 59761–59771, DOI: 10.1021/acsami.1c20548.

20 J. Wu, Z. Feng, C. Dong, P. Zhu, J. Qiu and L. Zhu, Synthesis of sodium carboxymethyl cellulose/poly(acrylic acid) microgels *via* visible-light-triggered polymerization as a self-sedimentary cationic basic dye adsorbent, *Langmuir*,

2022, **38**(12), 3711–3719, DOI: **10.1021/acs.langmuir.1c03196**.

21 R. Singh, V. Munya, V. N. Are, D. Nayak, S. Chattopadhyay and A. Biocompatible, pH-sensitive, and magnetically separable superparamagnetic hydrogel nanocomposite as an efficient platform for the removal of cationic dyes in wastewater treatment, *ACS Omega*, 2021, **6**(36), 23139–23154, DOI: **10.1021/acsomega.1c02720**.

22 S. B. Sengel and N. Sahiner, Poly(vinyl phosphonic acid) nanogels with tailored properties and their use for biomedical and environmental applications, *Eur. Polym. J.*, 2016, **75**, 264–275, DOI: **10.1016/J.EURPOLYMJ.2016.01.007**.

23 P. Gupta and R. Purwar, Influence of cross-linkers on the properties of cotton grafted poly(acrylamide-co-acrylic acid) hydrogel composite: swelling and drug release kinetics, *Iran. Polym. J.*, 2021, **30**(4), 381–391, DOI: **10.1007/S13726-020-00897-3/TABLES/4**.

24 G. R. Bardajee, R. Ghadimkhani and F. Jafarpour, A biocompatible double network hydrogel based on poly (acrylic acid) grafted onto sodium alginate for doxorubicin hydrochloride anticancer drug release, *Int. J. Biol. Macromol.*, 2024, **260**, 128871, DOI: **10.1016/J.IJBIOMAC.2023.128871**.

25 S. Roy, *et al.*, Design and development of novel urea, sulfonyltriurea, and sulfonamide derivatives as potential inhibitors of sphingosine kinase 1, *Pharmaceuticals*, 2020, **13**(6), 1–22, DOI: **10.3390/ph13060118**.

26 P. Ratrey, *et al.*, Emergent antibacterial activity of N-(thiazol-2-yl)benzenesulfonamides in conjunction with cell-penetrating octaarginine, *RSC Adv.*, 2021, **11**(46), 28581–28592, DOI: **10.1039/d1ra03882f**.

27 P. Ratrey, B. Datta and A. Mishra, Intracellular bacterial targeting by a thiazolyl benzenesulfonamide and octaarginine peptide complex, *ACS Appl. Bio Mater.*, 2022, **5**(7), 3257–3268, DOI: **10.1021/acsabm.2c00252**.

28 R. Choubey, M. Chatterjee, D. Johnson, V. Thiruvenkatam, A. Kumawat, A. Mishra and B. Datta, Tunable coassembly of octaarginine with thiazolyl benzenesulfonamides exerts variable antibacterial activity, *J. Phys. Chem. B*, 2024, **128**(3), 10434–10450, DOI: **10.1021/acs.jpcb.4c03336**.

29 P. Antonoaea, A. F. Miller, R.-A. Vlad, Z. R. Miladinovic, M. Krstic and E. Suljovrujic, Swelling behavior, biocompatibility, and controlled delivery of sodium–diclofenac in new temperature-responsive P(OEGMA/OPGMA) copolymeric hydrogels, *Gels*, 2025, **11**, 201, DOI: **10.3390/GELS11030201**.

30 G. Elyashevich, E. Rosova, Z. Zoolshoev, N. Saprykina and I. Kuryndin, Reversibility of swelling, pH sensitivity, electroconductivity, and mechanical properties of composites based on polyacrylic acid hydrogels and conducting polymers, *J. Compos. Sci.*, 2023, 7(6), 261, DOI: **10.3390/jcs7060261**.

31 S. A. nohooji, *et al.*, Chitosan/carbon quantum dots/polyvinylpyrrolidone nanocarrier for enhanced anticancer efficacy of doxorubicin, *Carbohydr. Polym. Technol. Appl.*, 2025, **11**, 100883, DOI: **10.1016/J.CARPTA.2025.100883**.

32 A. K. Barbary, M. A. Sallam, H. A. El-Maradny, D. A. Abdelmonsif, S. El-Achy and H. M. Helal, Dual-responsive hydrogel embedded with baricitinib loaded hydroxyapatite nanoparticles for local rheumatoid arthritis therapy, *J. Drug Deliv. Sci. Technol.*, 2025, **111**, 107141, DOI: **10.1016/J.JDDST.2025.107141**.

33 R. V. Pivato, F. Rossi, M. Ferro, F. Castiglione, F. Trotta and A. Mele, β-Cyclodextrin nanosponge hydrogels as drug delivery nanoarchitectonics for multistep drug release kinetics, *ACS Appl. Polym. Mater.*, 2021, **3**(12), 6562–6571, DOI: **10.1021/ACSAPM.1C01262/ASSET/IMAGES/MEDIUM/AP1C01262_M015.GIF**.

34 M. U. A. Khan, S. I. Abd Razaq, H. Mehboob, S. Rehman, W. S. Al-Arjan and R. Amin, Antibacterial and hemocompatible ph-responsive hydrogel for skin wound healing application: *in vitro* drug release, *Polymers*, 2021, **13**(21), 3703, DOI: **10.3390/polym13213703**.

35 E. V. Ramana, *et al.*, Ionically cross-linked pH-responsive hydrogel beads loaded with nickel cobaltite nanoparticles for controlled release of doxorubicin, *Colloid Polym. Sci.*, 2025, 1–10, DOI: **10.1007/S00396-025-05455-Y/FIGURES/3**.

36 M. Tsirigotis-Maniecka, L. Szyk-Warszyńska, Ł. Maniecki, W. Szczęsna, P. Warszyński and K. A. Wilk, Tailoring the composition of hydrogel particles for the controlled delivery of phytopharmaceuticals, *Eur. Polym. J.*, 2021, **151**, 110429, DOI: **10.1016/j.eurpolymj.2021.110429**.

37 T. Wan, Q. Zhang, G. Jin and S. Xu, Controlled delivery of 5-fluorouracil from monodisperse chitosan microspheres prepared by emulsion crosslinking, *RSC Adv.*, 2024, **14**(16), 11311–11321, DOI: **10.1039/D4RA01377H**.

38 S. Ata, *et al.*, Loading of Cefixime to pH sensitive chitosan based hydrogel and investigation of controlled release kinetics, *Int. J. Biol. Macromol.*, 2020, **155**, 1236–1244, DOI: **10.1016/J.IJBIOMAC.2019.11.091**.

39 A. Karimi-Rastehkenari, L. Youseftabar-Miri, E. Askarizadeh and F. Divsar, pH-sensitive magnetic nanocomposite hydrogels chitosan/hyaluronic acid/Fe_3O_4: ciprofloxacin release, kinetics and antibacterial activity, *Int. J. Biol. Macromol.*, 2025, 145211, DOI: **10.1016/J.IJBIOMAC.2025.145211**.

40 S. S. Abdullaev, R. H. Althomali, E. Abdu Musad Saleh, M. R. Robertovich, I. B. Sapaev, R. M. Romero-Parra, H. O. Alsaab, M. A. Gatea and M. N. Fenjan, Synthesis of novel antibacterial and biocompatible polymer nanocomposite based on polysaccharide gum hydrogels, *Sci. Rep.*, 2023, **13**(1), 16800, DOI: **10.1038/s41598-023-42146-6**.

41 Y. Pu, X. Lin, Q. Zhi, S. Qiao and C. Yu, Microporous implants modified by bifunctional hydrogel with antibacterial and osteogenic properties promote bone integration in infected bone defects, *J. Funct. Biomater.*, 2023, **14**(4), 226, DOI: **10.3390/jfb14040226**.

42 Á. Szegedi, *et al.*, Bicomponent drug formulation for simultaneous release of Ag and sulfadiazine supported on nanosized zeolite Beta, *Nano-Struct. Nano-Objects*, 2020, **24**, 100562, DOI: **10.1016/J.NANOSO.2020.100562**.

43 D. C. Morais, *et al.*, Combining polymer and cyclodextrin strategy for drug release of sulfadiazine from electrospun fibers, *Pharmaceutics*, 2023, **15**(7), 1890, DOI: 10.3390/PHARMACEUTICS15071890/S1.

44 L. Feng, H. Yang, X. Dong, H. Lei and D. Chen, pH-sensitive polymeric particles as smart carriers for rebar inhibitors delivery in alkaline condition, *J. Appl. Polym. Sci.*, 2018, **135**(8), 1–9, DOI: 10.1002/app.45886.

45 M. El-Sakhawy, A. Salama, S. Profile, S. Mohamed, and H.-A. Sarhan, *Carboxymethyl Cellulose Esters As Stabilizers For Hydrophobic Drugs In Aqueous Medium*, 2018, Available at: https://www.researchgate.net/publication/329877204.

46 E. M. Hussein, M. M. Al-Rooqi, A. A. Elkhawaga and S. A. Ahmed, Tailoring of novel biologically active molecules based on N4-substituted sulfonamides bearing thiazole moiety exhibiting unique multi-addressable biological potentials, *Arab. J. Chem.*, 2020, **13**(5), 5345–5362, DOI: 10.1016/j.arabjc.2020.03.014.

47 M. Suhail, P. C. Wu and M. U. Minhas, Development and characterization of pH-sensitive chondroitin sulfate-co-poly(acrylic acid) hydrogels for controlled release of diclofenac sodium, *J. Saudi Chem. Soc.*, 2021, **25**(4), 101212, DOI: 10.1016/j.jscs.2021.101212.

48 F. Jabbar, G. Abbas, N. Ameer, M. F. Akhtar, S. Shah and M. Hanif, Preparation and characterization of halloysite nanotubes containing hydrogels for controlled release drug delivery of cetirizine dihydrochloride, *Polym. Bull.*, 2022, **79**(7), 5417–5435, DOI: 10.1007/s00289-021-03750-6.

49 J. Yang, *et al.*, Curcumin-loaded pH-sensitive biopolymer hydrogels: fabrication, characterization, and release properties, *ACS Food Sci. Technol.*, 2022, **2**(3), 512–520, DOI: 10.1021/acsfoodscitech.1c00403.

50 K. Nagaraja, K. M. Rao, D. Hemalatha, S. Zo, S. S. Han and K. S. V. K. Rao, S*trychnos potatorum* L. seed polysaccharide-based stimuli-responsive hydrogels and their silver nanocomposites for the controlled release of chemotherapeutics and antimicrobial applications, *ACS Omega*, 2022, **7**(15), 12856–12869, DOI: 10.1021/acsomega.2c00131.

51 M. M. Ittisaf, M. Rakid-Ul-Haque, N. Tabassum, M. H. Pritom, M. S. H. Tanvir, M. A. Ali and S. Ahmed, Effect of the temperature of biomixing on the pH/temperature sensitive controlled drug release of a chitooligosaccharide-based hydrogel, *Mater. Adv.*, 2025, **6**, 4483–4498, DOI: 10.1039/D4MA01261E.

52 S. Huang, *et al.*, Development and characterization of biodegradable antibacterial hydrogels of xanthan gum for controlled ciprofloxacin release, *Int. J. Biol. Macromol.*, 2025, **309**, 142637, DOI: 10.1016/J.IJBIOMAC.2025.142637.

53 L. Lv, *et al.*, Poly(β-amino ester) dual-drug-loaded hydrogels with antibacterial and osteogenic properties for bone repair, *ACS Biomater. Sci. Eng.*, 2023, **9**(4), 1976–1990, DOI: 10.1021/acsbiomaterials.2c01524.

54 M. A. Alsakhawy, D. A. Abdelmonsif, M. Haroun and S. A. Sabra, Naringin-loaded Arabic gum/pectin hydrogel as a potential wound healing material, *Int. J. Biol. Macromol.*, 2022, **222**, 701–714, DOI: 10.1016/J.IJBIOMAC.2022.09.200.

55 R. S. H. Wong and K. Dodou, Effect of drug loading method and drug physicochemical properties on the material and drug release properties of poly(ethylene oxide) hydrogels for transdermal delivery, *Polymers*, 2017, **9**(7), 286, DOI: 10.3390/polym9070286.

56 A. J. R. Amaral, M. Emamzadeh and G. Pasparakis, Transiently malleable multi-healable hydrogel nanocomposites based on responsive boronic acid copolymers, *Polym. Chem.*, 2018, **9**(4), 525–537, DOI: 10.1039/c7py01202k.

57 K. Alam, M. Iqbal, A. Hasan and N. Al-Maskari, Rheological characterization of biological hydrogels in aqueous state, *J. Appl. Biotechnol. Rep.*, 2020, **7**(3), 172–176, DOI: 10.30491/jabr.2020.109994.

58 P. N. Dave, P. M. Macwan and B. Kamaliya, Synthesis and rheological investigations of gum-ghatti-cl-poly(NIPA-co-AA)-graphene oxide based hydrogels, *Mater. Adv.*, 2023, **4**(14), 2971–2980, DOI: 10.1039/d3ma00092c.

59 E. Giuliano, D. Paolino, M. C. Cristiano, M. Fresta and D. Cosco, Rutin-loaded poloxamer 407-based hydrogels for *in situ* administration: Stability profiles and rheological properties, *Nanomaterials*, 2020, **10**(6), 3–5, DOI: 10.3390/nano10061069.

60 R. E. Dey, I. Wimpenny, J. E. Gough, D. C. Watts and P. M. Budd, Poly(vinylphosphonic acid-co-acrylic acid) hydrogels: the effect of copolymer composition on osteoblast adhesion and proliferation, *J. Biomed. Mater. Res., Part A*, 2018, **106**(1), 255–264, DOI: 10.1002/jbm.a.36234.

61 G. Stojkov, Z. Niyazov, F. Picchioni and R. K. Bose, Relationship between structure and rheology of hydrogels for various applications, *Gels*, 2021, **7**(4), 255, DOI: 10.3390/gels7040255.

62 Y. Dong, *et al.*, Injectable and glucose-responsive hydrogels based on boronic acid-glucose complexation, *Langmuir*, 2016, **32**(34), 8743–8747, DOI: 10.1021/acs.langmuir.5b04755.

63 S. Heidari, M. Mohammadi, F. Esmaeilzadeh and D. Mowla, Determination of swelling behavior and mechanical and thermal resistance of acrylamide-acrylic acid copolymers under high pressures and temperatures, *ACS Omega*, 2021, **6**(37), 23862–23872, DOI: 10.1021/ACSOMEGA.1C02638.

64 S. Shin, S. Kim, S. Hong, N. Kim, J. Kang and J. Jeong, Tuning the swelling behavior of superabsorbent hydrogels with a branched poly(aspartic acid) crosslinker, *Gels*, 2025, **11**(3), 161, DOI: 10.3390/GELS11030161.

65 S. Morariu, M. Avadanei and L. E. Nita, Effect of pH on the poly(acrylic acid)/poly(vinyl alcohol)/lysozyme complexes formation, *Molecules*, 2024, **29**(1), 208, DOI: 10.3390/MOLECULES29010208/S1.

66 H. N. Öztop, F. Akyildiz and D. Saraydin, Poly(acrylamide/vinylsulfonic acid) hydrogel for invertase immobilization, *Microsc. Res. Tech.*, 2020, **83**(12), 1487–1498, DOI: 10.1002/jemt.23542.

67 M. M. H. Rumon, Advances in cellulose-based hydrogels: tunable swelling dynamics and their versatile real-time

applications, *RSC Adv.*, 2025, **15**(15), 11688–11729, DOI: 10.1039/D5RA00521C.

68 N. S. Malik, *et al.*, Chitosan/xanthan gum based hydrogels as potential carrier for an antiviral drug: fabrication, characterization, and safety evaluation, *Front. Chem.*, 2020, **8**, 510555, DOI: 10.3389/FCHEM.2020.00050/BIBTEX.

69 S. Jabeen, S. Alam, L. A. Shah, M. Zahoor, M. Naveed Umar and R. Ullah, Novel hydrogel poly (GG-co-acrylic acid) for the sorptive removal of the color rhodamine-B from contaminated water, *Heliyon*, 2023, **9**(9), e19780, DOI: 10.1016/J.HELIYON.2023.E19780.

70 X. Hong, H. Ding, J. Li, Y. Xue, L. Sun and F. Ding, Poly(acrylamide-co-acrylic acid)/chitosan semi-interpenetrating hydrogel for pressure sensor and controlled drug release, *Polym. Adv. Technol.*, 2021, **32**(8), 3050–3058, DOI: 10.1002/PAT.5317.

71 A. M. Elbarbary, M. M. Ghobashy, G. K. El Khalafawy, M. A. Salem and A. S. Kodous, Radiation cross-linking of pH-sensitive acrylic acid hydrogel based polyvinylpyrrolidone/2-dimethylamino ethyl methacrylate loaded with betamethasone dipropionate drug and *in vitro* anti-inflammatory assessment, *J. Drug Deliv. Sci. Technol.*, 2023, **89**, 105024, DOI: 10.1016/J.JDDST.2023.105024.

72 P. Jayachandran, *et al.*, Green synthesized silver nanoparticle-loaded liposome-based nanoarchitectonics for cancer management: *in vitro* drug release analysis, *Biomed*, 2023, **11**, 217, DOI: 10.3390/BIOMEDICINES11010217.

73 P. N. Dave, P. M. Macwan and B. Kamaliya, Biodegradable Gg-cl-poly(NIPAm-co-AA)/-o-MWCNT based hydrogel for combined drug delivery system of metformin and sodium diclofenac: *in vitro* studies, *RSC Adv.*, 2023, **13**(33), 22875–22885, DOI: 10.1039/d3ra04728h.

74 I. S. Bayer, Controlled drug release from nanoengineered polysaccharides, *Pharm*, 2023, **15**, 1364, DOI: 10.3390/PHARMACEUTICS15051364.

75 G. Cabrera Barjas, J. García-Couce, V. Gounden and M. Singh, Gold nanoparticle-based hydrogel: application in anticancer drug delivery and wound healing *in vitro*, *Pharm*, 2025, **17**, 633, DOI: 10.3390/PHARMACEUTICS17050633.

76 Z. S. Mohammadi, M. Pourmadadi, M. Abdouss, S. H. Jafari, A. Rahdar and A. M. Díez-Pascual, pH-sensitive polyacrylic acid/Fe_3O_4@SiO_2 hydrogel nanocomposite modified with agarose for controlled release of quercetin, *Inorg. Chem. Commun.*, 2024, **163**, 112338, DOI: 10.1016/J.INOCHE.2024.112338.

77 J. Phour and E. Vassella, Methods in cancer research: assessing therapy response of spheroid cultures by life cell imaging using a cost-effective live-dead staining protocol, *Biol. Methods Protoc.*, 2024, **9**(1), bpae060, DOI: 10.1093/BIOMETHODS/BPAE060.

78 J. Far, M. Abdel-Haq, M. Gruber and A. Abu Ammar, Developing biodegradable nanoparticles loaded with mometasone furoate for potential nasal drug delivery, *ACS Omega*, 2020, **5**(13), 7432–7439, DOI: 10.1021/acsomega.0c00111.

79 R. Li, *et al.*, Design and development of La(III) driven graphene oxide superabsorbent hydrogels from guar gum and gallic acid for drug delivery application: experimental and DFT evaluation, *New J. Chem.*, 2025, **42**, 3963–4776, DOI: 10.1039/D5NJ01279A.

80 Y.-X. Li and Y. Jiang, Synergistic occlusion of doxorubicin and hydrogels in CaCO3 composites for controlled drug release, *Crystals*, 2023, **13**(1), 132, DOI: 10.3390/cryst13010132.

81 Y. Liang, X. Zhao, P. X. Ma, B. Guo, Y. Du and X. Han, pH-responsive injectable hydrogels with mucosal adhesiveness based on chitosan-grafted-dihydrocaffeic acid and oxidized pullulan for localized drug delivery, *J. Colloid Interface Sci.*, 2019, **536**, 224–234, DOI: 10.1016/j.jcis.2018.10.056.

82 Z. Sayyar, G. R. Mahdavinia and A. Khataee, Dual-drug (curcumin/ciprofloxacin) loading and release from chitosan-based hydrogels embedded with magnetic montmorillonite/hyaluronic acid for enhancing wound healing, *J. Biol. Eng.*, 2023, **17**(1), 1–20, DOI: 10.1186/s13036-023-00385-1.

83 C. Yu, A. Naeem, Y. Liu and Y. Guan, Ellagic acid inclusion complex-loaded hydrogels as an efficient controlled release system: design, fabrication and *in vitro* evaluation, *J. Funct. Biomater.*, 2023, **14**(5), 278, DOI: 10.3390/jfb14050278.

84 R. Dwivedi, A. K. Singh and A. Dhillon, pH-responsive drug release from dependal-M loaded polyacrylamide hydrogels, *J. Sci. Adv. Mater. Dev.*, 2017, **2**(1), 45–50, DOI: 10.1016/j.jsamd.2017.02.003.